Protein Translation

DOI: 10.1002/ange.201300058

Suppression of Gene Expression by G-Quadruplexes in Open Reading Frames Depends on G-Quadruplex Stability**

*Tamaki Endoh, Yu Kawasaki, and Naoki Sugimoto**

Guanine-rich (G-rich) sequences of DNA form G-quadruplexes, a non-canonical structure stabilized by stacked G-quartets consisting of four guanine bases that interact through Hoogsteen-type hydrogen bonds.[1] G-quadruplexes have been studied from physical, chemical, and biological points of view because of their unique structure and stability under physiological conditions.[2,3] The best characterized G-quadruplex is that formed by the G-rich repeats of DNA at the ends of chromosomes, termed telomeres.[1] Because the telomere performs essential functions in chromosome maintenance and protection, the potential for G-quadruplex formation in telomere regions has potential importance for therapies. G-rich RNA can also form G-quadruplexes; these structures have higher melting temperatures than those formed by equivalent DNA sequences.[4–6] The high thermodynamic stability of RNA G-quadruplexes may affect various biological processes such as replication, transcription, and post-transcriptional editing.[7–12] Bioinformatic studies have revealed that sequences with quadruplex-forming potential (SQFPs) are found in the 5′ untranslated regions (UTRs) of oncogene mRNAs.[13] Because protein expression from these mRNAs decreases upon addition of G-quadruplex ligands and increases when mutations that disrupt the G-quadruplex formation are incorporated,[14–17] it is assumed that the quadruplex-forming sequences in the 5′ UTRs regulate protein-expression levels through formation of RNA G-quadruplexes.

In contrast to the effects of RNA G-quadruplexes in 5′ UTRs on gene expression, there is little information about G-quadruplexes in the open reading frames (ORFs) of mRNAs. One known difference between ORF and 5′ UTR regions during translation is that mature ribosomes, consisting of both small and large ribosomal subunits, progress along ORFs, whereas only the small ribosomal subunit complexed with the initiator tRNA scans the 5′ UTR before initiation of translation. It has been suggested that the mature ribosome in the elongation phase can unwind downstream duplexes in mRNAs more effectively than the small ribosomal subunit during the scanning phase.[18] Despite the helicase activity of the ribosome,[19,20] SQFPs are less abundant in ORFs than in UTRs in human mRNAs.[21] This observation suggests that G-quadruplexes might resist the helicase activity of the ribosome because its structure is different from a duplex or because it is highly thermodynamically stabile (which is further stabilized under conditions of molecular crowding), or both.[22–24] However, there is neither evidence of suppression of translation elongation mediated by the G-quadruplex nor information regarding how long and where the translation is suppressed. In this study, we therefore experimentally evaluated the effect of G-quadruplexes in ORFs on the translation reaction in vitro and in cells.

Previous reports studying the functions of G-quadruplexes have been focused on narrow SQFPs, which were picked from specified genes or model sequences.[7,9,16,17,25] Herein, we investigated the general effects of the SQFPs in ORFs on the translation reaction, all SQFPs of the form $G_XN_YG_XN_YG_XN_YG_X$, where G is guanine, N is any nucleotide, and $X = 3$–5 and $Y = 1$–5, were identified from the genomic sequence of the *E. coli* strain MG1655.[26] Five of the 38 SQFPs found were located within ORFs (Supporting Information, Table S1). RNA oligonucleotides containing SQFPs (wild-type) and their G-to-A mutants, in which the guanines from the potential G-quadruplex regions were replaced with adenines without changing the amino acid sequence, were prepared by in vitro transcription (Table S2 and Figure S1 a). We determined the UV melting profiles at 295 nm for these oligonucleotides in the presence of 40 wt% poly(ethylene glycol) with an average molecular weight of 200 (PEG200), which we have used to mimic intracellular conditions of reduced water because of osmolytes and macromolecules (Figure 1 a).[22,27] Because the melting temperatures in the presence of a physiological concentration (100 mM) of potassium were too high to quantitate the thermodynamic stabilities (data not shown), UV melting curves were obtained in a buffer containing 3 mM potassium. All the wild-type SQFPs had melting transitions typical of G-quadruplexes, while the G-to-A mutants did not show the same transition (data not shown). Formation of G-quadruplexes was also confirmed by partial digestion using RNase T1 (Figure 1 b). In the case of wild-type SQFPs, guanosines in the guanine-tracts (G-tracts) were considerably protected from RNase T1 digestion compared to those at the predicted loop regions (Figure 1 b, indicated by G_L). The G-tracts were most likely protected from RNase T1 digestion by forming G-quartets and stacking into quadruplexes. In contrast, for the G-to-A mutants, almost all guanosines (except in *glyQ*) were digested by RNase T1. Some guanosines in the G-to-A mutants of *glyQ* were protected through the formation of Watson–Crick

[*] T. Endoh, Y. Kawasaki, Prof. N. Sugimoto
Frontier Institute for Biomolecular Engineering Research (FIBER), Konan University
7-1-20 Minatojima-minamimachi, Kobe 650-0047 (Japan)
E-mail: sugimoto@konan-u.ac.jp

[**] Customized PURExfrex was kindly provided from GeneFrontier Corp. (http://www.genefrontier.com/english/index.html). This work was supported in part by Grants-in-Aid for Scientific Research and MEXT (Japan)-Supported Program for the Strategic Research Foundation at Private Universities (2009–2014).

Supporting information for this article is available on the WWW under http://dx.doi.org/10.1002/anie.201300058.

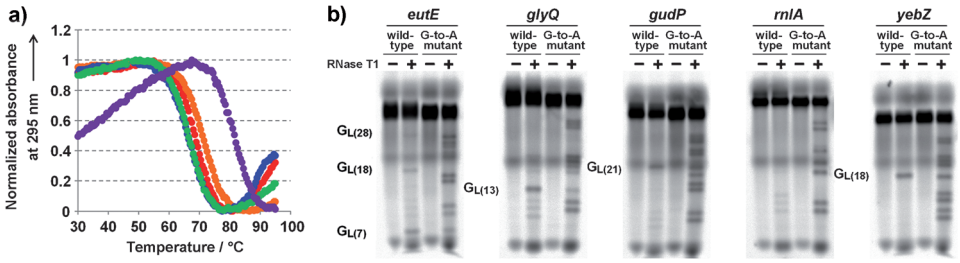

Figure 1. a) Normalized absorbance at 295 nm of 5 μM SQFPs derived from *eutE* (purple), *glyQ* (blue), *gudP* (red), *rnlA* (green), and *yebZ* (orange) in a buffer containing 50 mM MES-LiOH (pH 7.0), 3 mM KCl, and 40 wt% PEG200. UV melting was measured at a rate of 0.2 °C min^{-1}. b) Partial digestion of wild-type and G-to-A mutant sequences using RNase T1 (0.0025 U). The Alexa 546-labeled oligonucleotides were digested in buffer containing 50 mM MES-LiOH, pH 7.0, 3 mM KCl, and 40 wt% PEG200. Digested guanosines in the loop regions of quadruplexes (G_L) formed by wild-type SQFPs are shown. Numbers in parenthesis show the position within the sequences.

base pairs in their secondary structure (Figure S2). The thermodynamic stability at 37 °C ($\Delta G°_{37}$) of the RNA G-quadruplexes was calculated from the UV melting profiles using van't Hoff analysis (Table S3). The stability of the quadruplexes in 100 mM potassium ions would be higher than the values shown in Table S3. CD spectra of the wild-type SQFPs showed positive and negative peaks near 265 nm and 240 nm, respectively, that were larger than the peak intensities observed for the G-to-A mutant sequences (Figure S3). From these results, we concluded that the wild-type SQFPs formed parallel G-quadruplexes, in agreement with the previously suggested monomorphic property of RNA G-quadruplexes.[6,28]

The wild-type and G-to-A mutant sequences were inserted into a reporter mRNA encoding a T7-tag sequence followed by a UAG amber codon and 28 amino acids; these are referred to as wild-type and G-to-A mutant mRNAs (Figure S1 a). Formation of G-quadruplexes in the reporter mRNAs was confirmed by analysis of the fluorescence signal of protoporphyrin IX (PPIX), which specifically binds to parallel G-quadruplexes (Figure S1 b).[29] To evaluate the effect of G-quadruplexes formed within the ORFs of the reporter mRNAs on translation elongation, we used a synchronized translation assay that we developed to evaluate a single turnover of the elongation reaction.[30] The fluorescence signal of CR110-X-AF (a non-natural amino acid), which was incorporated into the translated products, in a 16% Tris-tricine SDS-PAGE gel was used to monitor translation elongation. In the lane from the reaction before translation was initiated (reaction time is zero), one main band was observed (indicated by H, Figure 2 a,b; Figure S4). Upon initiation of synchronized translation,[30] the wild-type mRNAs showed an intense band (indicated by I, Figure 2 a; Figure S4) that migrated slightly more slowly than the H band throughout the time course, up to 300 seconds. The signals observed at the same position of the H band are most likely a product that cannot be further elongated during the first reaction step due to inactivation of the ribosome.[30] For the G-to-A mutant mRNAs, the main fluorescence signal was observed near the 6.5 kDa marker after 60 seconds of the synchronized translation (indicated by F, Figure 2 b; Figure S4). The fluorescence signals indicated by I are intermediate products, because both the wild-type and G-to-A mutant mRNAs encode the same amino acid sequences (Figure S1 a). The longest products shown (F) are the full-length protein, in which the translation elongation progressed to the 3′ end of the mRNA, although the positions are slightly lower than expected; products of 6.6–6.9 kDa are produced from all of the mRNAs. The non-natural amino acid, CR110-X-AF, incorporated into the translated products, has a higher molecular weight than the natural amino acids and this likely affects the migration rate, because the parenchymal length of the full-length product is shorter than the natural protein having same molecular weight.

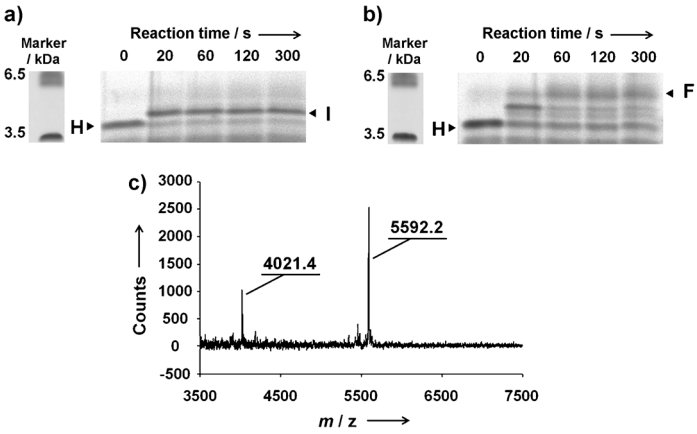

Figure 2. Time course of the synchronized translation of a) wild-type and b) G-to-A mutant mRNAs containing the *eutE* SQFP at their 3′ ends. Samples taken from the synchronized translation reactions at the indicated times were resolved on a 16% Tris-tricine SDS-PAGE gel. The CR110-X-AF signal was imaged using 473 nm excitation and 510 nm emission. c) Mass spectrometric analysis of the translated product of wild-type mRNA at 20 s from the restart of synchronized translation. The main observed mass signals are indicated.

To determine the stalling position of the ribosome on the wild-type mRNAs, translated products after 20 seconds from the translation restart were purified using anti-T7-tag agarose and their mass spectra were analyzed (Figure 2 c; Figure S5). For all of the mRNAs, the main mass signal was observed around 4022 *m*/*z* (4021.4, 4021.8, 4020.6, 4021.5, and 4024.8 for *eutE*, *glyQ*, *gudP*, *rnlA*, and *yebZ*, respectively) and 5592 *m*/*z* (5592.2, 5591.5, 5592.8, 5592.6, and 5591.6 for *eutE*, *glyQ*, *gudP*, *rnlA*, and *yebZ*, respectively). The signals around 4022 correspond to the translated product of the first reaction step of the synchronized translation; this product is a 29-residue peptide with an attached adenosine moiety,[30] which

has a calculated mass of 4022.3 *m*/*z* (Table S4), that is produced by artificial halt of the ribosome before the codon encoding tyrosine because of the absence of tyrosyl-tRNA synthetase in the reaction mixture. The signals around 5592 *m*/*z* correspond to a 42-residue peptide with an attached adenosine moiety, with a calculated mass of 5592.2 *m*/*z* (Table S4). In contrast to wild-type mRNAs, the mass spectra of the translated products from the G-to-A mutant mRNAs did not show the signal around 5592 *m*/*z* (data not shown). These results indicate that the translation elongation of wild-type mRNAs was stalled at the forty-second GGU codon for glycine (Figure S1 a).

Reporter vectors containing wild-type and G-to-A mutant sequences at the 5′ coding region of *Renilla* luciferase were co-transfected into a human breast carcinoma cell line (MCF7) and the human embryonic kidney cell line (Flp-In 293; Invitrogen) with the pSV40-FFL plasmid, which expresses firefly luciferase, and the relative luminescence units (RLU) of *Renilla* luciferase (RL) versus firefly luciferase (FFL) were determined (Figure 3; Figure S6). The RLUs

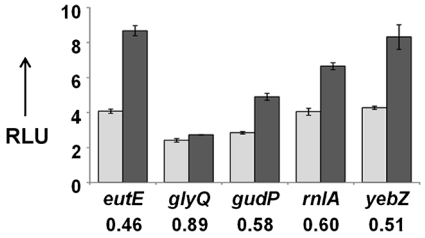

Figure 3. RLUs from *Renilla* luciferase versus firefly luciferase in MCF7 lysates. Reporter vector containing wild-type (light gray) or G-to-A mutant (dark gray) sequences at the 5′ coding region of *Renilla* luciferase was co-transfected with pSV40-FLuc. RLU ratios of wild-type SQFPs relative to G-to-A mutant sequences are indicated below the graph.

were lower in lysates from cells transfected with wild-type SQFPs compared to those with G-to-A mutant sequences. This indicates that *Renilla* luciferase expression was suppressed by the wild-type SQFP in the ORF. In both MCF7 and Flp-In 293 cells, RLU values of wild-type relative to those of G-to-A mutant indicated strong suppression (approximately 50%) by *eutE* and *yebZ* SQFPs, weaker suppression (10–20%) by *glyQ*, and moderate suppression (30–40%) by *gudP* and *rnlA* SQFPs. The relative RLU values varied with the ΔG°_{37} of the RNA G-quadruplexes; the SQFPs with more stable G-quadruplexes suppressed gene expression more efficiently (Table S3).

In this study, we selected SQFPs from ORFs of natural genes. When evaluated as oligonucleotides, each of the five SQFPs formed parallel G-quadruplexes. When the SQFPs were incorporated into an mRNA, translation elongation was stalled prior to the quadruplex-forming region. Using mass spectrometric analysis of the translated products, we determined that in a synchronized translation assay, the ribosome stalled six or seven nucleotides before the wild-type SQFPs (Figure S1 a). The crystal structure of the ribosome indicates that six nucleotides separate the A-site from the nucleotide located at the entry site of the mRNA into the ribosome.[31] Thus, when the ribosome is stalled, the forty-second GGU codon and the G-quadruplex formed by the SQFP are within the A-site and on the surface of the small ribosomal subunit, respectively. We hypothesize that the G-quadruplex structure blocks further entry of the mRNA into the ribosome because the diameter of the entry site (approximately 1.5 nm) is less than the diameter of the quadruplex (Figure 4).

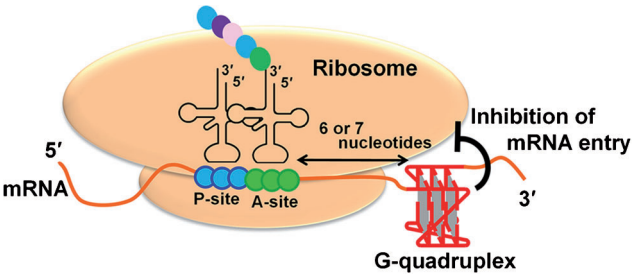

Figure 4. Scheme of the inhibition of translation elongation by G-quadruplexes at the surface of the 30S ribosome.

Intracellular expression of reporter genes containing wild-type SQFPs in an ORF was lower compared to expression from a reporter gene containing G-to-A mutant sequences. These data suggest that the RNA G-quadruplex structures in the ORF suppress the translation elongation, as was shown in the in vitro experiments. The suppression efficiencies were correlated with the thermodynamic stability of the RNA G-quadruplexes formed by the SQFPs. The strong suppression seen with the SQFPs derived from *eutE* and *yebZ* was comparable to previously reported suppression of gene expression by G-rich sequences in the 5′ UTRs.[14,16] Thus, despite the helicase activity of the ribosome,[20] RNA G-quadruplexes can suppress translation elongation by the mature ribosome, as well as scanning by the small ribosomal subunit. Because temporary stalling of translation elongation at specific positions can contribute to various biological actions, such as a ribosomal frameshift,[32] no-go mRNA decay,[33] and co-translational folding of nascent proteins,[34–37] quadruplex-forming ORFs may contribute to the regulation of these functions.

Experimental Section

Construction of RNAs: RNAs used in this study were prepared by in vitro transcription. DNA templates for in vitro transcription of short RNA oligonucleotides were constructed by primer extension using the T7 promoter primer and antisense primers, A (Table S5). DNA templates for reporter mRNAs were constructed by two-step PCR. First, DNA containing the sequence found in each of the reporter mRNAs was amplified by PCR from a plasmid vector, previously constructed for synchronized translation[30] using a T7 promoter primer and an antisense primer, B1 (Table S5). Second, DNA templates containing wild-type and G-to-A mutant SQFPs were amplified from the first PCR product using the T7 promoter primer and the respective antisense primers, B2 (Table S5). RNAs were transcribed using a ScriptMAX Thermo T7 Transcription Kit and purified by denaturing PAGE.

UV measurements: UV absorbance was measured with a Shimadzu-1800 UV/Vis spectrophotometer equipped with a temperature controller. Melting curves of 5 μM RNA oligonucleotides were obtained by measuring the UV absorbance at 295 nm in a buffer containing MES-LiOH (50 mM, pH 7.0), KCl (3 mM), and PEG200 (40 wt%). The heating rate was 0.2 °C min^{-1}. The thermodynamic stabilities at 37 °C ($\Delta G°_{37}$) were calculated from a fit of the melting curves to a theoretical equation for an intramolecular association as described previously.[23,38] Before the measurement, the samples were heated to 95 °C and cooled to 30 °C at a rate of 0.2 °C min^{-1}.

Partial digestion of RNA by RNase T1: RNA oligonucleotides were labeled with Alexa Fluor 546 C5-maleimide (Invitrogen) using the 5′ end-tag nucleic acid labeling system (Vector Laboratories). Labeled RNAs were purified in a denaturing polyacrylamide gel and precipitated with glycogen (20 μg) by ethanol precipitation. Labeled RNAs (5 pmol total) in buffer containing MES-LiOH (50 mM, pH 7.0), KCl (3 mM), and PEG200 (40 wt%) were incubated at 70 °C for 10 min and cooled to 37 °C at 1 °C min^{-1}, followed by 30 min incubation at 37 °C. The samples were incubated with RNase T1 (0.0025 U; Roche) at 37 °C for 10 min and electrophoresed on a 15% denaturing polyacrylamide gel at 70 °C. The fluorescence signal in the gel was imaged using a fluorescence image scanner (FLA-5100, Fuji Film) with 532 nm excitation and 575 nm emission.

Synchronized translation: Synchronized translation was performed using a reconstructed in vitro translation system[39,40] according to a previously published experimental procedure[30] with some modifications. All the reporter mRNAs were refolded by cooling from 90 °C to 4 °C at 1 °C min^{-1} in a buffer containing HEPES (30 mM, pH 6.8) and KCl (100 mM), and pre-incubated at 37 °C for 10 min. RF1, RF2, and TyrRS were removed from an in vitro translation system (PURExfrex; GeneFrontier), and the samples were pre-incubated at 37 °C for 10 min. An amber suppressor tRNA (CR110-X-AF-tRNAamber; Protein Ex-press) was added to the reaction mixture at final concentration of 1.6 μM. The first reaction was started by the addition of mRNA at a final concentration of 3.6 μM, and reaction mixture was incubated at 37 °C for 10 min. In the second reaction, an equal volume of the reaction mixture of PURExfrex containing all requisite proteins except ribosomes was pre-incubated at 37 °C for 10 min and then added to the reaction mixture of the first reaction to restart the translation elongation. Both the first and the second reactions were performed using the tRNA concentrations specified by the manufacturer; the absorbance at 260 nm of the tRNA mixture (A260/mltRNAmix) was 20. An aliquot of the restarted reaction mixture was quickly frozen in liquid nitrogen at the specified reaction time, and an equal volume of 4 M urea was added at 4 °C, followed by addition of RNase A and incubation at 37 °C for 10 min.

Gel electrophoresis of translated products: Translated products were resolved on a 16% Tris-tricine SDS-PAGE gel.[41] Fluorescence signals on the gel were imaged using a fluorescence image scanner with 473 nm excitation and 510 nm emission.

Mass spectrometry analysis: Translated products digested with RNase A were purified using anti-T7-tag agarose (MBL) as described.[30] The mass spectrum of the purified products was analyzed using MALDI-TOF mass spectrometry (Autoflex III, Bruker).

Construction of plasmids: The coding sequence of *Renilla* luciferase was excised from the pRL-SV40 plasmid (Promega) using *Nhe*I and *BamH*I restriction sites and cloned into *Xba*I and *BamH*I restriction sites of the pCMV-TnT vector (Promega) to make pCMV-TnT-RL. A DNA fragment containing the T7-tag sequence followed by *EcoR*I and *Sal*I restriction sites was amplified by PCR using oligonucleotide primers, C (Table S5). The DNA fragment was digested by *Xho*I and *BstB*I restriction enzymes, and cloned into the same sites of pCMV-TnT-RL to make pCMV-TnT-T7-RL. DNA fragments of the SQFPs were prepared by annealing sense and antisense oligonucleotides, D (Table S5) and cloned into *EcoR*I and *Sal*I restriction sites of pCMV-TnT-T7-RL to make the reporter plasmids containing the SQFPs in the ORF (pCMV-TnT-T7-QFP-RL). The coding sequence of firefly luciferase was excised from the PicaGene Control Vector 2 (Toyo Ink) using *Hind*III and *Xba*I restriction enzymes and was cloned into the same restriction sites of pRL-SV40 to make pSV40-FFL.

Cell culture and transfection: Media used for culturing MCF7 and Flp-In 293 cells were EMEM and DMEM, respectively. The media were supplemented with fetal bovine serum (10%) and antibiotics (penicillin, 100 U mL^{-1} and streptomycin, 100 μg mL^{-1}). Cells were maintained at 37 °C under 5% CO_2. Cells were plated on collagen-coated 96 well plates at a density of 1×10^4 cells per well and incubated overnight. Vector pCMV-TnT-T7-QFP-RL (50 ng) was co-transfected with pSV40-FFL (5 ng) into cells using X-tream GENE 9 (0.3 μL, Roche) according to the manufacturer's directions.

Luciferase assay: Cells were lysed in a passive lysis buffer (Promega) 24 h after transfection. Cell lysate (10 μL) was transferred to a white 384 well plate. Luminescence signals of FFL and RL in the lysate were measured by the Dual-Glo Luciferase Assay System (Promega) with a multispectral microwell plate reader (Varioskan Flash; Thermo Scientific).

Received: January 4, 2013
Revised: March 4, 2013
Published online: April 15, 2013

Keywords: G-quadruplexes · open reading frames · protein translation · RNA recognition · thermodynamic stability

[1] J. R. Williamson, *Annu. Rev. Biophys. Biomol. Struct.* **1994**, *23*, 703 – 730.
[2] G. W. Collie, G. N. Parkinson, *Chem. Soc. Rev.* **2011**, *40*, 5867 – 5892.
[3] J. E. Johnson, J. S. Smith, M. L. Kozak, F. B. Johnson, *Biochimie* **2008**, *90*, 1250 – 1263.
[4] A. Arora, S. Maiti, *J. Phys. Chem. B* **2009**, *113*, 10515 – 10520.
[5] A. Joachimi, A. Benz, J. S. Hartig, *Bioorg. Med. Chem.* **2009**, *17*, 6811 – 6815.
[6] D. H. Zhang, T. Fujimoto, S. Saxena, H. Q. Yu, D. Miyoshi, N. Sugimoto, *Biochemistry* **2010**, *49*, 4554 – 4563.
[7] V. Marcel, P. L. Tran, C. Sagne, G. Martel-Planche, L. Vaslin, M. P. Teulade-Fichou, J. Hall, J. L. Mergny, P. Hainaut, E. Van Dyck, *Carcinogenesis* **2010**, *32*, 271 – 278.
[8] W. I. Sundquist, S. Heaphy, *Proc. Natl. Acad. Sci. USA* **1993**, *90*, 3393 – 3397.
[9] I. Kuzmine, P. A. Gottlieb, C. T. Martin, *Nucleic Acids Res.* **2001**, *29*, 2601 – 2606.
[10] P. H. Wanrooij, J. P. Uhler, T. Simonsson, M. Falkenberg, C. M. Gustafsson, *Proc. Natl. Acad. Sci. USA* **2010**, *107*, 16072 – 16077.
[11] V. Marcel, P. L. Tran, C. Sagne, G. Martel-Planche, L. Vaslin, M. P. Teulade-Fichou, J. Hall, J. L. Mergny, P. Hainaut, E. Van Dyck, *Carcinogenesis* **2011**, *32*, 271 – 278.
[12] D. Gomez, T. Lemarteleur, L. Lacroix, P. Mailliet, J. L. Mergny, J. F. Riou, *Nucleic Acids Res.* **2004**, *32*, 371 – 379.
[13] S. G. Hershman, Q. Chen, J. Y. Lee, M. L. Kozak, P. Yue, L. S. Wang, F. B. Johnson, *Nucleic Acids Res.* **2008**, *36*, 144 – 156.
[14] K. Halder, M. Wieland, J. S. Hartig, *Nucleic Acids Res.* **2009**, *37*, 6811 – 6817.
[15] S. Kumari, A. Bugaut, J. L. Huppert, S. Balasubramanian, *Nat. Chem. Biol.* **2007**, *3*, 218 – 221.
[16] S. Kumari, A. Bugaut, S. Balasubramanian, *Biochemistry* **2008**, *47*, 12664 – 12669.
[17] M. Wieland, J. S. Hartig, *Chem. Biol.* **2007**, *14*, 757 – 763.
[18] M. Kozak, *Mol. Cell. Biol.* **1989**, *9*, 5134 – 5142.
[19] X. Qu, J. D. Wen, L. Lancaster, H. F. Noller, C. Bustamante, I. Tinoco, Jr., *Nature* **2011**, *475*, 118 – 121.
[20] S. Takyar, R. P. Hickerson, H. F. Noller, *Cell* **2005**, *120*, 49 – 58.

[21] J. L. Huppert, S. Balasubramanian, *Nucleic Acids Res.* **2005**, *33*, 2908 – 2916.
[22] D. Miyoshi, T. Fujimoto, N. Sugimoto, *Top. Curr. Chem.* **2012**, *330*, 87 – 110.
[23] D. Miyoshi, H. Karimata, N. Sugimoto, *J. Am. Chem. Soc.* **2006**, *128*, 7957 – 7963.
[24] S. Pramanik, S. Nagatoishi, N. Sugimoto, *Chem. Commun.* **2012**, *48*, 4815 – 4817.
[25] D. Gomez, A. Guedin, J. L. Mergny, B. Salles, J. F. Riou, M. P. Teulade-Fichou, P. Calsou, *Nucleic Acids Res.* **2010**, *38*, 7187 – 7198.
[26] F. R. Blattner, G. Plunkett III, C. A. Bloch, N. T. Perna, V. Burland, M. Riley, J. Collado-Vides, J. D. Glasner, C. K. Rode, G. F. Mayhew, J. Gregor, N. W. Davis, H. A. Kirkpatrick, M. A. Goeden, D. J. Rose, B. Mau, Y. Shao, *Science* **1997**, *277*, 1453 – 1462.
[27] M. M. Garner, M. B. Burg, *Am. J. Physiol.* **1994**, *266*, C877 – 892.
[28] A. Y. Zhang, A. Bugaut, S. Balasubramanian, *Biochemistry* **2011**, *50*, 7251 – 7258.
[29] T. Li, E. Wang, S. Dong, *Anal. Chem.* **2010**, *82*, 7576 – 7580.
[30] T. Endoh, Y. Kawasaki, N. Sugimoto, *Anal. Chem.* **2012**, *84*, 857 – 861.
[31] L. Jenner, P. Romby, B. Rees, C. Schulze-Briese, M. Springer, C. Ehresmann, B. Ehresmann, D. Moras, G. Yusupova, M. Yusupov, *Science* **2005**, *308*, 120 – 123.
[32] D. P. Giedroc, P. V. Cornish, *Virus Res.* **2009**, *139*, 193 – 208.
[33] M. K. Doma, R. Parker, *Nature* **2006**, *440*, 561 – 564.
[34] A. A. Komar, *Trends Biochem. Sci.* **2009**, *34*, 16 – 24.
[35] E. P. O'Brien, S. T. Hsu, J. Christodoulou, M. Vendruscolo, C. M. Dobson, *J. Am. Chem. Soc.* **2010**, *132*, 16928 – 16937.
[36] G. Zhang, Z. Ignatova, *Curr. Opin. Struct. Biol.* **2010**, *20*, 25 – 31.
[37] E. P. O'Brien, M. Vendruscolo, C. M. Dobson, *Nat. Commun.* **2012**, *3*, 868.
[38] L. A. Marky, K. J. Breslauer, *Biopolymers* **1987**, *26*, 1601 – 1620.
[39] Y. Shimizu, T. Kanamori, T. Ueda, *Methods* **2005**, *36*, 299 – 304.
[40] Y. Shimizu, A. Inoue, Y. Tomari, T. Suzuki, T. Yokogawa, K. Nishikawa, T. Ueda, *Nat. Biotechnol.* **2001**, *19*, 751 – 755.
[41] H. Schägger, *Nat. Protoc.* **2006**, *1*, 16 – 22.

